

Available online at www.sciencedirect.com

ScienceDirect

journal homepage: <http://www.elsevier.com/locate/medici>

Original Research Article

Scaffold design for artificial tissue with bone marrow stem cells

Aurelija Noreikaitė^a, Ieva Antanavičiūtė^b, Valeryia Mikalayeva^b, Adas Darinskas^c, Tomas Tamulevičius^d, Erika Adomavičiūtė^e, Linas Šimatonis^d, Dalia Akramienė^a, Edgaras Stankevičius^{a,*}

^aInstitute of Physiology and Pharmacology, Medical Academy, Lithuanian University of Health Sciences, Kaunas, Lithuania

^bInstitute of Cardiology, Medical Academy, Lithuanian University of Health Sciences, Kaunas, Lithuania

^cLaboratory of Immunology, National Cancer Institute, Vilnius, Lithuania

^dInstitute of Materials Science, Kaunas University of Technology, Kaunas, Lithuania

^eFaculty of Mechanical Engineering and Design, Kaunas University of Technology, Kaunas, Lithuania

ARTICLE INFO

Article history:

Received 23 January 2017

Received in revised form

26 June 2017

Accepted 3 July 2017

Available online 13 July 2017

Keywords:

Biological pacemaker

Scaffold

Stem cells

Bone marrow

Polyimide film

ABSTRACT

Objective: The aim of this study was to test polymeric materials (collagen, fibrin, polyimide film, and polylactic acid) for single- and multi-layer scaffold formation.

Materials and methods: In our study, we used rabbit bone marrow stem cells (rBMSCs) and human mesenchymal stem cells (hMSCs) with materials of a different origin for the formation of an artificial scaffold, such as a collagen scaffold, fibrin scaffold produced from clotted rabbit plasma, electrospun poly(lactic acid) (PLA) mats, polyimide film (PI), and the combination of the latter two. Cell imaging was performed 3–14 days after cell cultivation in the scaffolds. Time-lapse imaging was used to determine hMSC mobility on the PI film.

Results: Cell incorporation in collagen and clotted fibrin scaffolds was evaluated after 2-week cultivation in vitro. Histological analysis showed that cells penetrated only external layers of the collagen scaffold, while the fibrin clot was populated with rBMSCs through the entire scaffold thickness. As well, cell behavior on the laser micro-structured PI film was analyzed. The mobility of hMSCs on the smooth PI film and the micro-machined surface was $20 \pm 2 \mu\text{m/h}$ and $18 \pm 4 \mu\text{m/h}$, respectively. After 3-day cultivation, hMSCs were capable of spreading through the whole $100 \pm 10 \mu\text{m}$ -thick layer of the electrospun PLA scaffold and demonstrated that the multilayer scaffold composed of PI and PLA materials ensured a suitable environment for cell growth.

Conclusions: The obtained results suggest that electrospinning technology and femtosecond laser micro-structuring could be employed for the development of multi-layer scaffolds. Different biopolymers, such as PLA, fibrin, and collagen, could be used as appropriate environments for cell inhabitation and as an inner layer of the multi-layer scaffold. PI could

* Corresponding author at: Institute of Physiology and Pharmacology, Medical Academy, Lithuanian University of Health Sciences, A. Mickevičiaus 9, 44307 Kaunas, Lithuania.

E-mail address: edgaras.stankevicius@ismuni.lt (E. Stankevičius).

<http://dx.doi.org/10.1016/j.medici.2017.07.001>

1010-660X/© 2017 The Lithuanian University of Health Sciences. Production and hosting by Elsevier Sp. z o.o. This is an open access article under the CC BY-NC-ND license (<http://creativecommons.org/licenses/by-nc-nd/4.0/>).

be suitable as a barrier blocking cell migration from the scaffold. However, additional studies are needed to determine optimal parameters of inner and outer scaffold layers.

© 2017 The Lithuanian University of Health Sciences. Production and hosting by Elsevier Sp. z o.o. This is an open access article under the CC BY-NC-ND license (<http://creativecommons.org/licenses/by-nc-nd/4.0/>).

1. Introduction

The field of stem cell therapy and tissue engineering is rapidly developing for a wide range of applications. Current therapies include bone regeneration, treatment of insulin delivery disorders [1,2], and cardiovascular and nervous tissue repair [3–6]. Scaffolds are used as drug delivery systems or as a base for cells in tissue engineering [7]. Artificial polymeric scaffolds serve as an extracellular matrix substitute for cell adhesion, proliferation, and differentiation. Artificial scaffolds developed from different type of materials using various fabrication techniques should meet the following requirements: (1) to be biocompatible with cells; (2) to be nontoxic (polymer and its degradation products); (3) to have good mechanical properties and flexibility; (4) to have controlled biodegradability; (5) to have an easily formed porous structure; (6) to have appropriate thermoplastic properties [8,9]. Moreover, communication between grafted cells and the neighboring tissue should be ensured [4,10]. Potential scaffold materials are classified as natural (collagen, gelatin, fibrin, alginate, etc.) and synthetic polymers (polylactic glycolic acid, polyurethane, polycaprolactone, etc.) [11]. Conventional fabrication techniques (e.g., gas foaming, salt leaching, freeze-drying, etc.) are widely used for designing artificial scaffolds. The main disadvantage of these scaffold fabrication techniques is that they cannot enable precise architecture of a 3D scaffold pore; moreover, cell viability can also be affected by the presence of toxic solvents if they are not completely removed [12]. Electrospinning is one of the alternative approaches. It is a simple, cost-effective, and versatile technique that allows formation of biocompatible nano-fibrous scaffolds for tissue engineering. Nano- or micro-fibrous mats can be deposited on various substrates, including a grounded metal plate, dielectric materials, and even the human body [13,14].

Deposited mats can also be lithographically patterned [15] and even dry etched in plasma [16], ablated with an ultra-fast laser [17,18], or transferred on other substrates using micro-contact printing [16].

To the best of our knowledge, electrospinning on ultra-fast laser micro-machined polyimide (PI) film substrates has not been performed so far; however, the use of the Kapton film [19,20] or even the polyimide polymer solution itself [21] for electrospinning has already been reported.

In the present study, differently fabricated scaffolds were tested with rabbit bone marrow stem cells (rBMSCs) and human mesenchymal stem cells (hMSCs) for the formation of an artificial scaffold: collagen sponge, fibrin clot, micro-structured PI film, and electrospun poly(lactic acid) (PLA) mats. Furthermore, a multi-layer scaffold designed from micro-structured PI and electrospun PLA mats was investigated.

2. Materials and methods

2.1. Cells

rBMSCs were derived directly from the rabbit bone sacrum by puncture using an 18G needle, syringe, and 0.02 mg/mL heparin (Sigma–Aldrich, Germany) solution as an anticoagulant. Bone marrow suspension was centrifuged using Ficoll–Paque density gradient; mononuclear cell fractions were placed into T25 tissue flasks (Orange scientific, Belgium) in Dulbecco's Modified Eagle Medium (DMEM) (Sigma–Aldrich, Germany) supplemented with 15% fetal calf serum (FCS, Gibco, USA), and the cells were cultivated with antibiotics (penicillin 100 U/mL and streptomycin 100 µg/mL, Sigma–Aldrich, Germany) at 37 °C and 5% CO₂. After 2-week cultivation, only stem cells were left as an adherent culture.

The license for the use of laboratory animals (No. 0171, 31-10-2007) was received from the Lithuanian Food and Veterinary Service.

hMSCs (Lonza, USA) were cultured at 37 °C in humidified 5% CO₂ atmosphere using BD Mosaic™ hMSC Culture Medium with supplement (Lonza, USA).

2.2. Scaffolds

In our study, we used commercially available bovine type I collagen sponge (Southern Lights Biomaterials, UK), fibrin produced from clotted rabbit plasma, several combinations of commercially available 12.7-µm thickness Kapton® 50HN PI film (DuPont™, Wilmington, DE, USA) and electrospun PLA (Nature Works, USA) mats (4% PLA electrospun solution in chloroform solvent was prepared). Scaffold structures were visualized by employing a scanning electron microscope (SEM) Quanta 200 FEG (FEI, Hillsboro, Oregon, USA).

Air bubble-free scaffolds were placed on tissue culture plates (5 cm) covered with 2% low melting agarose (Sigma, Germany) and DMEM where niches for implants were formed. Then, scaffolds were placed in these niches, and the cells were gently introduced into them using a syringe and a 21G needle (~2 × 10⁶ rBMSCs per 0.5 × 0.5-cm scaffold).

rBMSCs were introduced into the fibrin scaffolds by the clot formation technology. Rabbit plasma was collected into heparinized tubes and separated from cells by centrifugation at 1500 × g for 15 min. Before polymerization, plasma was mixed with differentiated cells cultured in the growth medium (DMEM, 10% FCS). For 1 mL of the final mixture, we used 2.5 × 10⁶ of live cells. After cell addition, the mixture was gently stirred and left until clotted. Five minutes after cell-fibrin scaffold formation, the mixture was gently introduced on a 12-well tissue culture plate.

Collagen and fibrin-cell scaffolds were maintained in DMEM with 10% FCS and antibiotics (penicillin 100 U/mL, streptomycin 100 µg/mL) and supplemented with 0.5 ng/mL TGFβ (Sigma-Aldrich, Germany). The medium was changed every 3 days. Cell persistence in the scaffolds was examined histologically 2 weeks after cell seeding.

Free standing electrospun mats, PI films with micrometer hole arrays as well as a PI supporting grid structure with electrospun PLA polymer microfiber mat were investigated. Holes in the PI films were micro-machined employing 4 W average power Yb:KGW femtosecond laser Pharos (Light Conversion, Vilnius, Lithuania) and FemtoLAB micro-machining workstation (Altechna R&D, Vilnius, Lithuania). The sample was placed on the motorized XYZ translation stages and positioned with respect to the microscope objective-focused 515-nm wavelength (second harmonic) laser beam. The polymer microfiber mat on the PI supporting grid structure was deposited from PLA by employing Nanospider™ (Elmarco, Liberec, Czech Republic) electrospinning setup. The laser structured PI films were sewed on the polypropylene spun-bonded non-woven substrate. Polymer jets from Taylor cones are formed when created electrostatic forces exceed surface tension of a polymer solution. Polymer jets split to microfibers while moving to a grounded electrode covered by a PI film on the substrate. Electrospun mats from PLA microfibers were formed under the following conditions: applied voltage 50 kV, distance between electrodes 13 cm, environmental temperature 20 °C ± 2 °C, humidity 60% ± 5%, and electrospun microfibers collection time 3 min. More details about the employed techniques for the later scaffold fabrication can be found elsewhere [12].

hMSC were grown on the PI film, PLA, and PLA-PI film scaffolds under conditions described above. For time-lapse recordings, 2×10^5 cells were seeded on the PI film. PLA-PI film scaffolds were seeded with 2×10^6 hMSCs and cultivated under the same conditions.

2.3. Histological analysis

Scaffolds with cells were cut with a microtome and set to the standard preparation procedures. Histological analysis of collagen and fibrin cell-scaffold sections was performed using Axio Imager Z1 (Carl Zeiss, Germany) and software AxioVision 4.7.1 (Carl Zeiss, Germany). The slices were stained with hematoxylin/eosin and were analyzed under a light microscope.

2.4. Cell imaging

hMSCs were grown for 3 days in the scaffolds (PLA, PI film, and PLA-PI film) and then labeled with CellMask™ Deep Red plasma membrane stain and Hoechst 33342 (Molecular Probes, USA) according to the manufacturer's protocols. Images were acquired using an Olympus IX81 microscope (Olympus Europe holding GmbH, Germany) and an Orca-R2 digital camera (Hamamatsu Photonics K.K., Japan) with the fluorescence excitation system MT10 and XCELLENCE software (Olympus Soft Imaging Solutions GmbH, Germany). Cell mobility measurements were performed at 37 °C in a humidified atmosphere of 5% CO₂ using an incubation system

INUBG2E-ONICS (Tokai Hit, Japan) with an incubator, mounted on the stage of the motorized Olympus IX81 microscope.

2.5. Statistical analysis

Data analysis was performed using SigmaPlot software (Systat, USA), and the data are presented as mean ± SE. Statistical analysis was performed using the Student t test. Differences were considered statistically significant at $P < 0.05$.

3. Results

3.1. Cell penetration in fibrin clot and solid-state collagen scaffolds

The penetration rate of rBMSCs within the collagen sponge and the fibrin clot was investigated (Fig. 1). Cells were grown in vitro and survived in the scaffolds for 2 weeks. Histological analysis (Fig. 1B) revealed that 90% of the cells resided in the zone of the external collagen scaffold layer. The average cell infiltration depth was 400 ± 45 µm. Fig. 1D indicates that rBMSCs occupied the entire volume of the 3D fibrin scaffold formed by the clot formation technique.

3.2. Cell behavior on micro-machined PI

Previously described scaffolds (Fig. 1) with the varying size of pores formed by disorderly arranged fibrin and collagen fibers had limited applications to some extent. It is possible that cells could escape to the neighboring environment from such an implanted collagen or fibrin scaffold. Development of a multi-layer scaffold with an impermeable outer layer could be a proper solution to overcome this limitation. However, sufficient nutrient transfer to the internal layers of the multi-layer scaffold should be ensured. For that purpose, PI films with micrometer hole arrays were investigated. Femtosecond laser ablation was employed to obtain a micro-structured pattern, i.e. a porous grid, in the PI film with precise dimensions (Fig. 2).

hMSCs were grown on the smooth and micro-machined PI film (Fig. 3), and the impact of surface differences on cell mobility was evaluated. Mobility of hMSCs on the smooth PI and laser micro-machined PI film was 20 ± 2 µm/h ($n = 50$) and 18 ± 4 µm/h ($n = 50$), respectively.

3.3. Development of a multi-layer scaffold

Further investigations were directed to fabrication of a multi-layer scaffold by combining two techniques: electrospinning and laser micro-machining. Free-standing electrospun mats could be used for production of an inner layer of the scaffold and provide a proper environment for cell inhabitation. These composite electrospun mats can be produced from a wide range of polymeric solutions. The main advantages of such a scaffold, e.g., composed from PLA, are controlled mat density of the surface area for cell attachment and high porosity, which enable persistent nutrition uptake. In this study, we tested PI films with micrometer hole arrays and electrospun PLA polymer microfiber mat (Fig. 4).

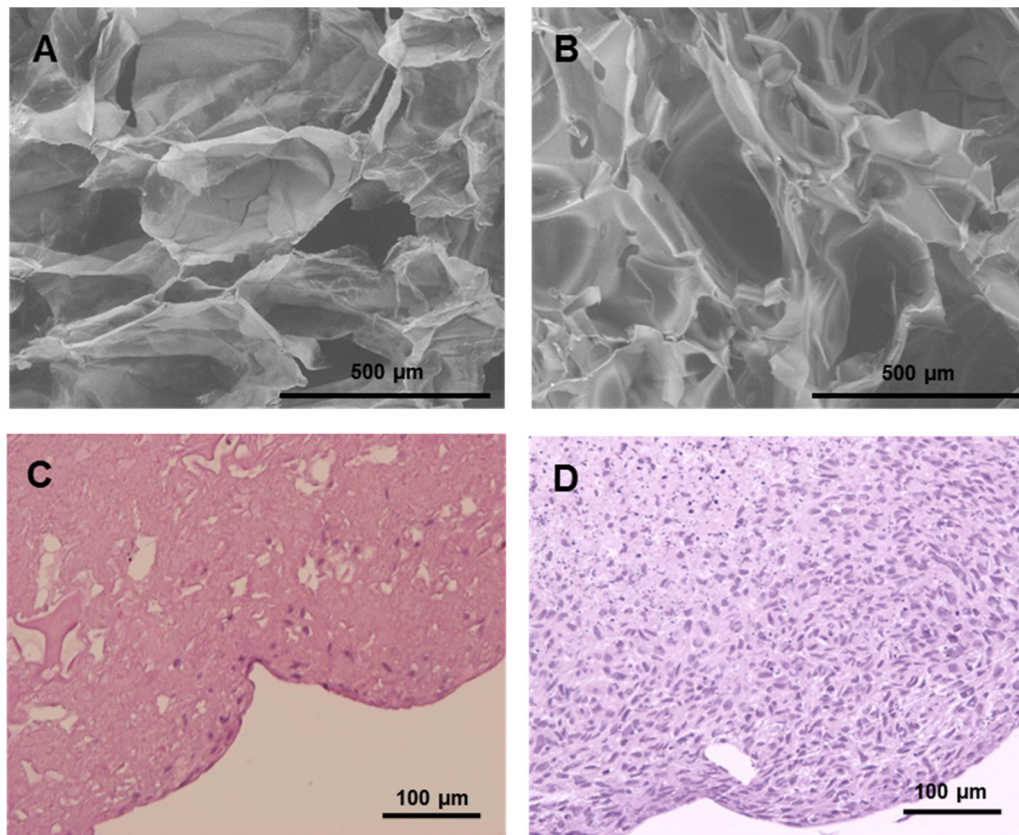


Fig. 1 – Cell incorporation in the collagen scaffold and the fibrin clot. SEM images of polymerized collagen (A) and fibrin scaffolds (B). Hematoxylin-eosin staining of collagen (C) and fibrin (D) scaffolds introduced with rBMSCs.

At the beginning of the deposition process, the PI film was firstly covered by a thinner layer of PLA microfibers, and later on when the mat became thicker, the diameter of the deposited microfibers increased. The diameter of electrospun PLA microfibers varied from $0.22\ \mu\text{m}$ to $17\ \mu\text{m}$, due to quick evaporation of the chloroform solvent in the PLA solution.

Comparative analysis of the multi-layer (PLA-PI) scaffold specimens revealed the dependence of PLA fiber mat density

on the micro-structured PI film pattern (Fig. 4). More fibers (approximately by 40%) were deposited on the same area of the PI film with micro-machined holes of $100 \times 100\ \mu\text{m}$ (Fig. 4A) compared with mats on the PI film with a few micrometer diameter hole array (Fig. 4B).

Our results showed that hMSCs were capable to spread through the whole $100 \pm 10\text{-}\mu\text{m}$ PLA scaffold thickness after 3-day cultivation (Fig. 5B). Fig. 5B, D, F demonstrates that both

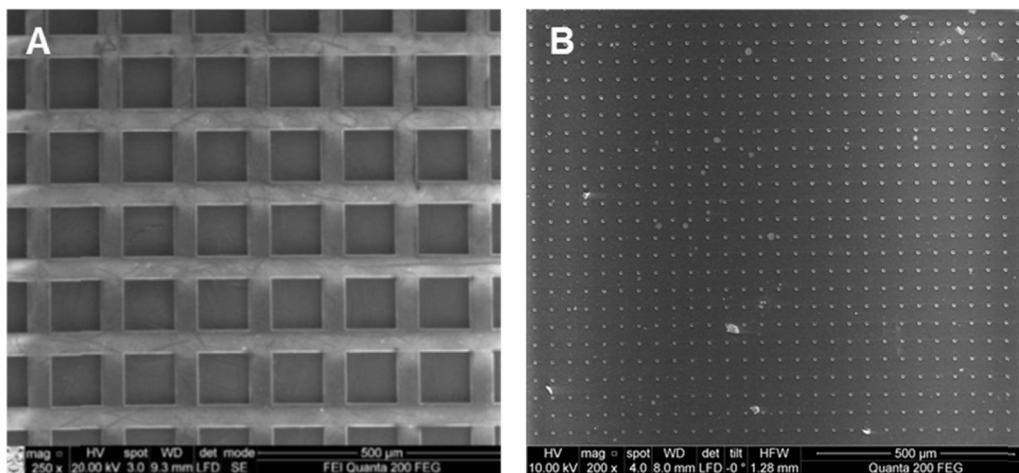


Fig. 2 – SEM images of laser micro-machined holes in the PI film. The regularly arranged grid of $100 \times 100\ \mu\text{m}$ (A) and $4\text{-}\mu\text{m}$ diameter (B) holes in the PI film.

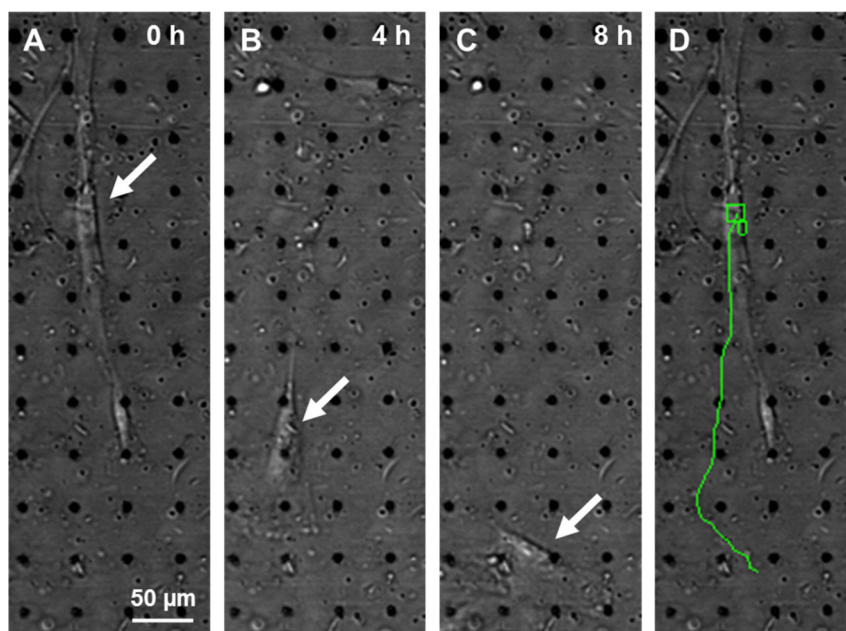


Fig. 3 – hMSC mobility on the micro-structured PI film. Images of a migrating cell (indicated by the white arrow) at different time points (0, 4, and 12 h) (A-C); (D) estimation of the cell trajectory (green line) using XCELLENCE software.

single materials PI or PLA as well as the multi-layer scaffold composed of PI and PLA materials ensured a suitable environment for cell growth.

4. Discussion

In order to reduce cell migration and to provide an appropriate environment for the regeneration of tissues and organs, 3D porous scaffolds were investigated. Scaffold design as well as initial cell infusion should meet certain requirements: biocompatibility (i), biodegradability (ii), mechanical properties in consistent with implantation site (iii), interconnected

pore structure and high porosity to ensure cellular penetration and adequate diffusion (iv), and cost effective manufacturing technology (v) [22].

Procedures of cell implantation may be improved by applying injectable (e.g., fibrin gels or fibrin as naturally clot-forming protein) and solid-state forms of artificial scaffolds as cell carriers. In the present study, differently processed collagen and fibrin scaffolds were investigated. Cells were seeded into collagen sponges, whereas the clot formation technique was applied for the construction of 3D cell-fibrin scaffold derivatives. The obtained differences at the cell penetration level in these two scaffolds were mainly determined by the cell-scaffold complex formation technique. After

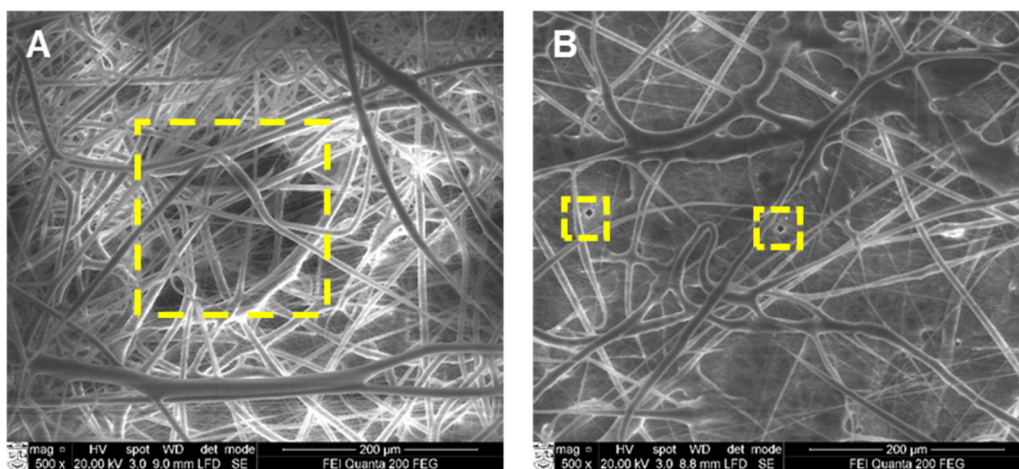


Fig. 4 – SEM micrographs of electrospun PLA fibers on the micro-structured PI film. PLA mats deposited on the PI film with a regularly arranged grid of 100 × 100 μm (A) and 4-μm diameter (B) holes (yellow dotted lines depict holes structured on the PI film).

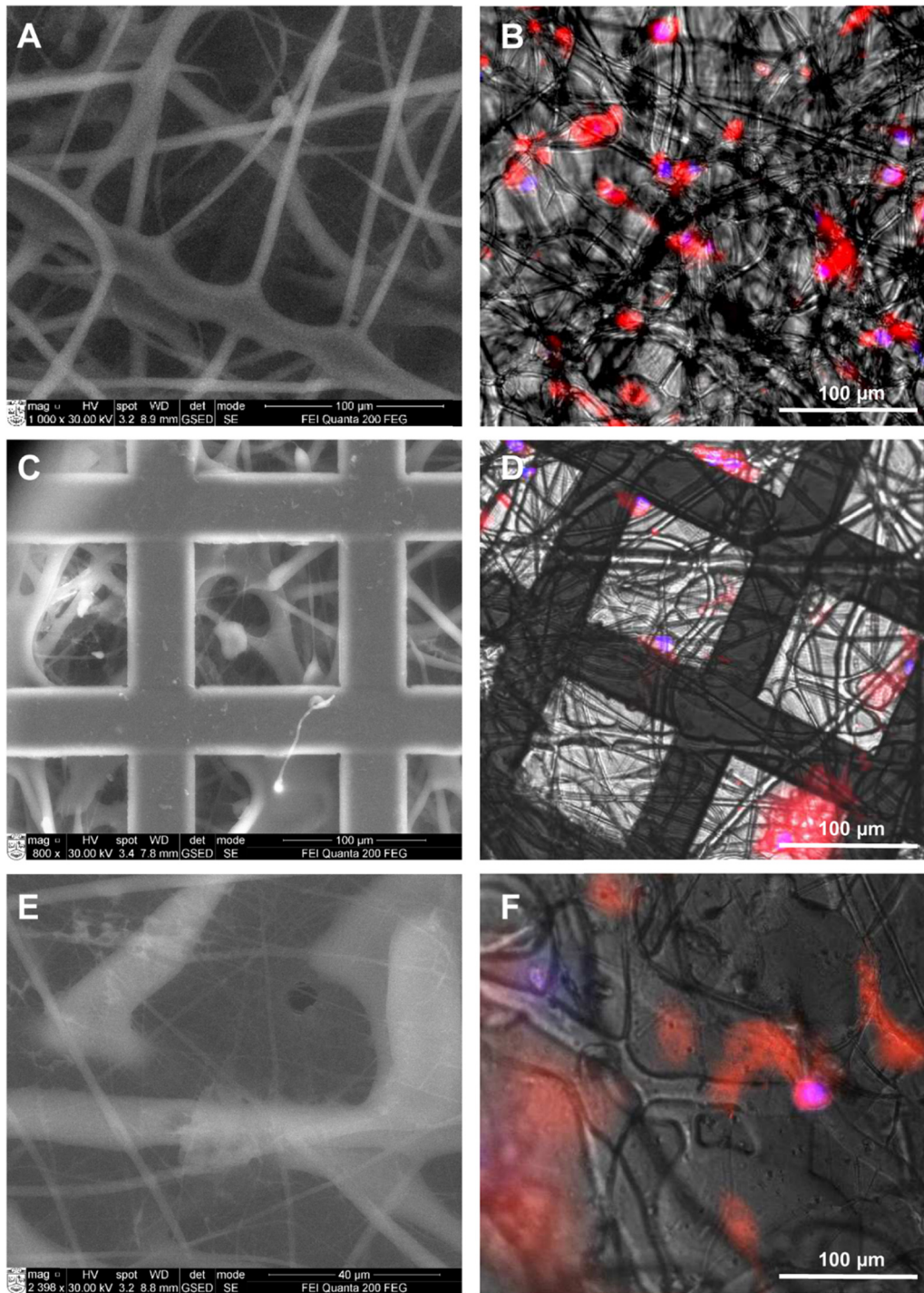


Fig. 5 – hMSC incorporation into the scaffolds of different architecture. Morphology of electrospun PLA fibers (A), and two-layer scaffolds of PLA fibers and the PI film with micro-structured holes (C, E). (B, D, F) hMSC in the scaffolds 3 days after the seeding (red – plasma membrane stained with CellMask™ Deep Red stain; blue – nuclei stained with Hoechst 33342).

2-week cultivation, rBMSCs were observed only on the external surface of the collagen scaffold, while the entire fibrin clot was occupied by rBMSCs. Our results indicate that different techniques may enhance scaffold inhabitation by cells. However, primary sufficient cell incorporation and survival

in the scaffold is limited by its thickness, as a result of inconsistent oxygen and nutrient transfer to the deeper levels.

The common feature of the previously described scaffolds is disorderly arranged pores. Variable pore sizes enable cells to escape from such structures and to migrate from the

implantation site to the neighboring environment that may lead to the loss of function. This is extremely important to avoid unexpected effects for the applications where cells have to be maintained at the implantation site. The aim of this study was to design a multi-layer scaffold. The micro-machined PI film, which was reported as biocompatible material [23,24], was chosen for the outer layer formation. Laser processing of polymers can induce some defects, i.e., thermal damage via melting and vaporization as well as morphological changes that can be minimized by shortening the laser pulse length [25]. Even with a femtosecond laser, the wetting properties of surfaces can still be altered by surface texturing and nano- and/or micro-textures could be generated, depending on the chosen processing parameters. Moreover, wetting is often anisotropic due to anisotropy of the laser-induced micro- and nano-structures. The wetting properties of PI depend on micro- and nano-structures generated during laser ablation [26]. For that purpose, time-lapse experiments with hMSC were performed on the laser micro-machined and smooth PI film. Our results revealed that hMSC mobility was not influenced by the examined surfaces and suggested PI as a proper material for the design of the semi-permeable (permeable for nutrition uptake and impermeable for cell trans-migration) outer scaffold layer.

PLA free-standing electrospun mats were tested for the development of the internal part of the multi-layer scaffold. In the present study, we evaluated the penetration of cells through $\sim 100 \mu\text{m}$ PLA mats. One of the main challenges in tissue engineering applications that needs to be overcome is limited cell colonization throughout pores, since pores have a varying size and are too small or too large between fibers [27,28]. Different methods are being used (salt leaching, gas foaming, etc.) for manipulating electrospun scaffold structures in order to increase the pore size or loosen the scaffold. The pore size and the fiber diameter also strongly correlate, where a reduction in the diameter of the fiber reduces the pore size of the meshes, which hinders cell infiltration or migration. It is difficult to separate the interdependence of the pore size and the fiber diameter and, therefore, to obtain a scaffold with nano- or micro-scale fibers but with macro-scale pores (10–500 μm). There are many parameters affecting electrospinning fiber diameters: deposition conditions, polymers properties (conductivity, viscosity), solvent system and its properties. By increasing the dielectric constant of the solvent, the final fiber diameter can be decreased in the same electrospinning conditions. The polarity of the solution is another important factor in reducing the final fiber diameter. The porosity of electrospun material increases while the fiber diameter is decreasing [29–31]. The pore size can be controlled by using patterned electrodes [32] or “templating” with insulating [29] or conductive [29,33] collectors. Under a strong electric field, insulating substrates can be polarized, which could consequently affect the distribution of the original electric field. Electrospun fibers can be attracted to the protrusions of the appropriate insulating substrates, due to opposite charges generated by static induction and polarization on protrusions [32]. Our findings with laser micro-machined insulating PI carriers are in agreement with those of other authors [32], where it was reported that fewer fibers were deposited in the non-conductive hole, i.e., insulating

protrusions, as its diameter decreased. At the same time, fiber density decreased. An opposite behavior was observed when conductive substrates were used [29]. The diameter of electroconductive wires and the combination of protrusions, other parameters, such as dimensions and spacings of protrusions, as well as wire spacings in woven collectors, may also affect the interactions between fibers and collectors, which can further influence the patterning of fibers [33].

The proposed technique combining precise micro-machining of designed porosity substrates/carriers together with high throughput fiber deposition via electrospinning enables control of the cells and penetration of nutrition to the scaffold structure. At the same time, it affects deposition of the polymer fiber mesh due to an impact on the local electric field variations induced by the dielectric PI mesh carriers. The designed PLA fibrous mesh as well as the multi-layer scaffold made of micro-machined PI and electrospun PLA mesh provided a suitable environment for cell growth.

5. Conclusions

The obtained results suggest that electrospinning technology and femtosecond laser micro-structuring could be employed for the development of a multi-layer scaffold. Different biopolymers as PLA, fibrin, and collagen could be used as appropriate environments for cell inhabitation. PI could be suitable as a barrier blocking cell migration from a scaffold. However, additional studies are needed to determine optimal parameters of inner and outer scaffold layers.

Conflict of interests

The authors have no conflict of interest to declare.

Acknowledgments

The study was supported by a financial grant from the European Social Fund project BOKARDIOSTIM VP1-3.1-ŠMM-10-V-02-029.

REFERENCES

- [1] Marchioli G, van Gurp L, van Krieken PP, Stamatialis D, Engelse M, van Blitterswijk CA, et al. Fabrication of three-dimensional bioplotting hydrogel scaffolds for islets of Langerhans transplantation. *Biofabrication* 2015;7:025009.
- [2] Moore SJ, Gala-Lopez BL, Pepper AR, Pawlick RL, Shapiro AMJ. Bioengineered stem cells as an alternative for islet cell transplantation. *World J Transplant* 2015;5:1–10.
- [3] Tyler B, Gullotti D, Mangraviti A, Utsuki T, Brem H. Polylactic acid (PLA) controlled delivery carriers for biomedical applications. *Adv Drug Deliv Rev* 2016;107:163–75.
- [4] Polymeric scaffolds in tissue engineering application: a review. *Int J Polym Sci* 2011;2011.

- [5] Chang HM, Wang ZH, Luo HN, Xu M, Ren XY, Zheng GX, et al. Poly(3-hydroxybutyrate-co-3-hydroxyhexanoate)-based scaffolds for tissue engineering. *Braz J Med Biol Res* 2014;47:533–9.
- [6] Xu XY, Li XT, Peng SW, Xiao JF, Liu C, Fang G, et al. The behaviour of neural stem cells on polyhydroxyalkanoate nanofiber scaffolds. *Biomaterials* 2010;31:3967–75.
- [7] Garg T, Singh O, Arora S, Murthy R. Scaffold: a novel carrier for cell and drug delivery. *Crit Rev Ther Drug Carrier Syst* 2012;29:1–63.
- [8] Hutmacher DW. Scaffolds in tissue engineering bone and cartilage. *Biomaterials* 2000;21:2529–43.
- [9] Hollister SJ. Porous scaffold design for tissue engineering. *Nat Mater* 2005;4:518–24.
- [10] Bryant SJ, Anseth KS. Controlling the spatial distribution of ECM components in degradable PEG hydrogels for tissue engineering cartilage. *J Biomed Mater Res A* 2003;64:70–9.
- [11] Wang F, Guan J. Cellular cardiomyoplasty and cardiac tissue engineering for myocardial therapy. *Adv Drug Deliv Rev* 2010;62:784–97.
- [12] Loh QL, Choong C. Three-dimensional scaffolds for tissue engineering applications: role of porosity and pore size. *Tissue Eng B: Rev* 2013;19:485–502.
- [13] Kenawy el R, Layman JM, Watkins JR, Bowlin GL, Matthews JA, Simpson DG, et al. Electrospinning of poly(ethylene-co-vinyl alcohol) fibers. *Biomaterials* 2003;24:907–13.
- [14] Kai D, Prabhakaran MP, Jin G, Ramakrishna S. Guided orientation of cardiomyocytes on electrospun aligned nanofibers for cardiac tissue engineering. *J Biomed Mater Res B: Appl Biomater* 2011;98:379–86.
- [15] Sharma CS, Sharma A, Madou M. Multiscale carbon structures fabricated by direct micropatterning of electrospun mats of SU-8 photoresist nanofibers. *Langmuir* 2010;26:2218–22.
- [16] Shi J, Wang L, Chen Y. Microcontact printing and lithographic patterning of electrospun nanofibers. *Langmuir* 2009;25:6015–8.
- [17] Adomavičiūtė E, Tamulevičius T, Šimatonis L, Fataraitė-Urbonienė E, Stankevičius E, Tamulevičius S. Microstructuring of electrospun mats employing femtosecond laser. *Mater Sci* 2015;21.
- [18] Götze M, Krimig O, Kürbitz T, Henning S, Heilmann A, Hillrichs G. Processing of polyamide electrospun nanofibers with picosecond UV-laser irradiation. *Phys Proc* 2016;83:147–56.
- [19] Zheng Y, Cheng L, Yuan M, Wang Z, Zhang L, Qin Y, et al. An electrospun nanowire-based triboelectric nanogenerator and its application in a fully self-powered UV detector. *Nanoscale* 2014;6:7842–6.
- [20] Liu N, Fang G, Wan J, Zhou H, Long H, Zhao X. Electrospun PEDOT: PSS-PVA nanofiber based ultrahigh-strain sensors with controllable electrical conductivity. *J Mater Chem* 2011;21:18962–6.
- [21] Nah C, Han SH, Lee M-H, Kim JS, Lee DS. Characteristics of polyimide ultrafine fibers prepared through electrospinning. *Polym Int* 2003;52:429–32.
- [22] O'Brien FJ. Biomaterials & scaffolds for tissue engineering. *Mater Today* 2011;14:88–95.
- [23] Julien S, Peters T, Ziemssen F, Arango-Gonzalez B, Beck S, Thielecke H, et al. Implantation of ultrathin, biofunctionalized polyimide membranes into the subretinal space of rats. *Biomaterials* 2011;32:3890–8.
- [24] Antanavičiūtė I, Šimatonis L, Ulčinis O, Gadeikytė A, Abakevičienė B, Tamulevičius S, et al. Femtosecond laser micro-machined polyimide films for cell scaffold applications. *J Tissue Eng Regen Med* 2016. <http://dx.doi.org/10.1002/term.2376>
- [25] Morikawa J, Orié A, Hashimoto T, Juodkazis S. Thermal diffusivity in femtosecond-laser-structured micro-volumes of polymers. *Appl Phys A* 2010;98:551–6.
- [26] Guo XD, Dai Y, Gong M, Qu YG, Helseth LE. Changes in wetting and contact charge transfer by femtosecond laser-ablation of polyimide. *Appl Surf Sci* 2015;349:952–6.
- [27] Declercq HA, Desmet T, Dubrue P, Cornelissen MJ. The role of scaffold architecture and composition on the bone formation by adipose-derived stem cells. *Tissue Eng A* 2014;20:434–44.
- [28] Sobral JM, Caridade SG, Sousa RA, Mano JF, Reis RL. Three-dimensional plotted scaffolds with controlled pore size gradients: effect of scaffold geometry on mechanical performance and cell seeding efficiency. *Acta Biomater* 2011;7:1009–18.
- [29] Vaquette C, Cooper-White JJ. Increasing electrospun scaffold pore size with tailored collectors for improved cell penetration. *Acta Biomater* 2011;7:2544–57.
- [30] Wu J, Hong Y. Enhancing cell infiltration of electrospun fibrous scaffolds in tissue regeneration. *Bioactive Mater* 2016;1:56–64.
- [31] Entekhabi E, Haghbin Nazarpak M, Moztarzadeh F, Sadeghi A. Design and manufacture of neural tissue engineering scaffolds using hyaluronic acid and polycaprolactone nanofibers with controlled porosity. *Mater Sci Eng: C* 2016;69:380–7.
- [32] Zhao S, Zhou Q, Long Y-Z, Sun G-H, Zhang Y. Nanofibrous patterns by direct electrospinning of nanofibers onto topographically structured non-conductive substrates. *Nanoscale* 2013;5:4993–5000.
- [33] Zhang D, Chang J. Patterning of electrospun fibers using electroconductive templates. *Adv Mater* 2007;19:3664–7.